This is a repository copy of *Measurement of Particle Concentration in Settling Multiphase Pipe Flow Using Acoustic Methods*.

White Rose Research Online URL for this paper:
http://eprints.whiterose.ac.uk/111298/

Version: Accepted Version

Proceedings Paper:

Measurement of particle concentration in settling multiphase pipe flow using acoustic methods

H.P. Rice[1], M. Fairweather[1], T.N. Hunter[1], B. Mahmoud[1], S.R. Biggs[1] and J. Peakall[2]

[1]School of Process, Environmental and Materials Engineering
[2]School of Earth and Environment
University of Leeds, Leeds LS2 9JT, UK

h.p.rice@leeds.ac.uk

1 Introduction

The transport and mixing behaviour of particles in turbulent, multiphase flows is of great interest in a wide range of engineering industries because of the effect of the suspended particles on flow parameters such as pressure drop and delivered mass of solids, and the influence on operability through plugging, flow constriction and corrosion, for example.

In this study, a model developed by marine scientists that relates the backscattered acoustic signal received by an active transducer in the megahertz range to the properties of the particles in a suspension (Thorne and Hanes, 2002) has been adapted to allow the measurement of the attenuation and backscatter coefficients for arbitrary suspensions of solid particles with the aim of using these coefficients in the dual-frequency inversion method (Hurther *et al.*, 2011) for engineering applications. This method circumvents many of the problems inherent in other inversion methods but requires fore-knowledge of these acoustic coefficients.

The received root-mean-square (RMS) voltage, V, varies with distance, r, from the transducer in which it is excited, as follows (Thorne and Hanes, 2002):

$$V = \frac{k_s k_t}{\psi r} M^{1/2} e^{-2r\alpha}, \qquad (1)$$

where k_s is the backscatter coefficient, k_t is a system constant, ψ is a near-field correction factor, M is the particle concentration by mass and α is the attenuation per unit distance, with components for water and suspended particles, α_w and α_s, respectively, such that

$$\alpha = \alpha_w + \alpha_s. \qquad (2)$$

In a homogeneous suspension, *i.e.* one in which the concentration and particle size distribution (PSD) do not vary with distance,

$$\alpha_s = \xi_h M, \qquad (3)$$

where ξ_h is the attenuation coefficient in the homogeneous case.

A novel method for determining ξ_h and K_h for particle species of any material (rather than marine sediment, the only material for which values of ξ_h and K_h have been published; see Thorne and Meral, 2008) was presented by Rice *et al.* (2014) and is briefly reiterated here. Some algebraic manipulation of Eq. (1) yields the following:

$$\frac{\partial}{\partial M}\left(\frac{\partial}{\partial r}[\ln(\psi rV)]\right) = -2\xi_h. \qquad (4)$$

Once ξ_h is known, the backscatter and system constant in the homogeneous case, K_h, which is defined as follows:

$$K_h = k_{sh} k_t, \qquad (5)$$

can be calculated by rearrangement of Eq. (1), that is:

$$K_h = \psi V M^{-1/2} \exp[2r(\alpha_w + \xi_h M)]. \qquad (6)$$

These coefficients can then be used to construct particle concentration profiles in any homogeneous or heterogeneous suspension *via* the dual-frequency inversion method (Hurther et al., 2011) in which M is found using the following expression:

$$M = J_1^{(1-\xi_1/\xi_2)^{-1}} J_2^{(1-\xi_2/\xi_1)^{-1}} \qquad (7)$$

where J is defined as follows:

$$J = V^2/\Phi^2, \qquad (8)$$

and the subscripts correspond to each ultrasonic frequency. V is the measured voltage and Φ^2 consists of the known variables in Eq. (1), *i.e.*

$$\Phi^2 = \left(\frac{K_h}{\psi r}\right)^2 \exp(-4\alpha_w r). \qquad (9)$$

The power of this method lies in the fact that it can be applied to any suspension (provided the attenuation is not excessive) so that the effects of flow rate on the segregation and settling behaviour can be observed directly. It can also be used in optically opaque suspensions and is straightforward to implement. To demonstrate the method as a whole, particle concentration profiles are presented in horizontal turbulent pipe flow at Re ≈ 45,000 – *i.e.* non-settling flows – at three nominal volume fractions (ϕ_w = 0.5, 1 and 3 %) for four particle species (two spherical glass and two non-spherical plastic).

In addition, novel methods for determining the critical deposition velocity, U_c – which separates settling and non-settling flows – and the thickness of settled particle beds are briefly described. Results gathered using these methods are combined with concentration profiles at Re ≈ 25,000 – below the critical deposition velocity – for two example cases, one in a slightly attenuating suspension of glass spheres, and another in a strongly attenuating suspension of plastic beads, with the aim of fully characterising the structure of some model multiphase flows and observing the crucial influence of acoustic attenuation.

2 Methodology

In this section, the various methods employed in this study are described in the following order. Section 2.1: acoustic coefficient measurement; section 2.2: settled bed depth measurement; section 2.3: critical deposition velocity measurement.

A commercially available ultrasonic measurement system (*UVP-DUO*, Met-Flow, Switzerland) and custom MATLAB scripts (MathWorks, USA) were used to calculate the intensity of the signal backscattered by suspended particles. Two spherical glass and two non-spherical plastic particle types were used (Guyson International Ltd., UK; mean diameters d_{50} = 41, 77, 468 and 691 µm, determined using *Mastersizer 2000* and *3000*, Malvern Instruments). The system-applied gain and digitisation constant were removed from the data, and a three-sigma noise filter was applied.

2.1 Acoustic coefficients measurement

Homogeneous suspensions of known concentrations were produced in a stirred mixing vessel, and ξ_h and K_h at two ultrasonic frequencies (2 and 4 MHz) were measured. Data from the same two transducers mounted on a horizontal test section of a recirculating pipe loop with an inner diameter of 42.6 mm carrying suspensions of the same particles were then generated and combined using Eq. (7) (in which J_1, J_2 and M are functions of distance, r), and concentration profiles along a vertical cross-section were constructed. Physical samples were also taken, for validation purposes. The experimental procedure has been described in more detail by Rice *et al.* (2014).

The measured values of ξ_h and K_h are presented in Table 1. All values are well within an order of magnitude of estimates based on quartz sand (not shown here; see Thorne and Hanes, 2002, and Rice *et al.*, 2014) and increase with particle size and frequency, as expected: ξ_h and K_h are proportional to $(ka)^4$ and $(ka)^2$, respectively, at low ka (*i.e. ka* < 1) and reach constant values at high ka (*i.e. ka* > 10), where k is the ultrasonic wavenumber ($k = 2\pi/\lambda$) and a is the mean particle diameter (for more details, see Thorne and Hanes, 2002).

Table 1: Measured values of ξ_h and K_h at 2 and 4 MHz.		
	2 MHz	4 MHz
Small glass (d_{50} = 41 µm)		
ka	0.174	0.348
ξ_h	0.0182	0.0694
K_h	0.00229	0.00430
Large glass (d_{50} = 77 µm)		
ka	0.327	0.654
ξ_h	0.0212	0.135
K_h	0.00363	0.00700
Small plastic (d_{50} = 468 µm)		
ka	1.99	3.97
ξ_h	0.627	2.74
K_h	0.0100	0.0239
Large plastic (d_{50} = 691 µm)		
ka	2.93	5.87
ξ_h	1.34	2.73
K_h	0.0163	0.0182

2.2 Settled bed depth measurement

The received RMS echo voltage, V, exhibits a strong peak at a reflective surface. This property of the acoustic measurement system employed in the present study was used not only to calibrate the position of the 4 MHz transducer – mounted perpendicular to the flow direction and also, therefore, the lower pipe wall, at which a strong reflection was observed – but also to measure the position of the upper surface of settled particle beds at the bottom of the pipe cross-section following cessation of the flow (during a "stop-flow" run).

Then, the bed depth could be calculated by subtraction of the position of the bed surface from the known position of the lower pipe wall.

The method is explained in more detail in Rice (2013), and some examples are shown in Section 4.

2.3 Critical velocity measurement

An unambiguous method for determining the critical deposition velocity, U_c, in solid-liquid suspensions was developed by Rice (2013), and is outlined here for the purpose of justifying the choice of runs chosen for presentation.

As described in Section 2.2, the depth of settled particle beds can be measured using the local peak in the RMS echo voltage, V, because a bed acts as a reflective surface. The method of settled bed depth measurement consists of a number of stages: (a) a bed of measurable thickness (in practice, at least several millimetres, as the resolution of the *UVP-DUO* instrument at the frequencies used in this study is of the order of a fraction of a millimetre) is generated by running the flow loop at a low flow rate for several minutes so that particles deposit in the test section; (b) the flow velocity is increased by a small increment, and the bed depth, which is subject to the competing mechanisms of particle deposition by gravity and erosion by the flow, is allowed to equilibrate over several seconds to minutes; (c) the flow is ceased, and the bed depth measured using the perpendicular (4 MHz) transducer; (d) a correction to the bed depth for would-be suspended sediment is made; and (e) the critical velocity (*x*-axis) is calculated by extrapolation of the bed depth (*y*-axis) over a range of flow velocities as that at which the bed depth is zero (*i.e.* at the intercept with the *x*-axis). The accuracy of the method was estimated to be ±5 %.

For the purpose of justifying the categorisation of non-settling (Section 3) and settling (Section 4) flows presented here, values of Re_c, the Reynolds number corresponding to U_c, are given in Table 2.

Table 2: Critical deposition Reynolds numbers, Re_c. From Rice (2013).

Particle type	ϕ_w (%)		
	0.5	1	3
Small glass	19,200	26,000	30,000
Large glass	26,600	29,700	35,300
Small plastic	30,600	33,700	39,100
Large plastic	33,200	37,300	46,900

3 Results: Non-settling flows

Concentration profiles at Re ≈ 45,000 at several nominal concentrations, ϕ_w, in the pipe loop for each of the four particle species are presented in Figure 1 (small glass particles), Figure 2 (large glass), Figure 3 (small plastic) and

Figure 4 (large plastic). Note that the axes in those figures are orientated so as to aid visualisation. With reference to Table 2, it is clear that all runs presented in this section fall into the non-settling category, as Re > Re_c (with the exception of the results for the large plastic particle species at ϕ_w = 3 %).

As expected, M/M_w increases with distance from the upper pipe wall due to settling. There are clear peaks near the pipe bottom, indicating strong segregation and the formation of moving and stationary beds. However, it is generally underestimated relative to the nominal concentration, M_w, which is thought to be caused by deposition in the mixing tank and elsewhere in the flow loop.
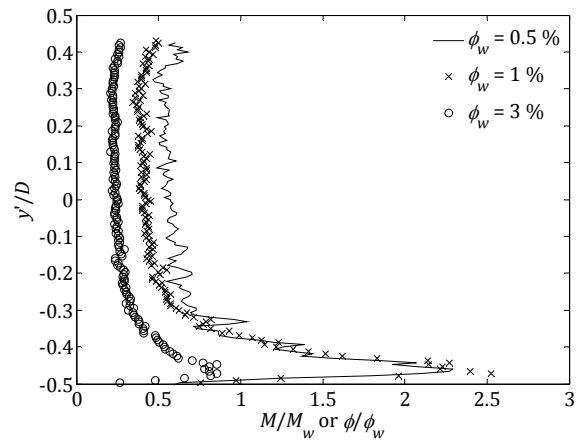

Figure 1: Particle concentration versus distance from centreline (normalised) with small glass spheres (d_{50} = 41 μm) at three nominal (weighed) concentrations. Re = 45,900, 45,600 and 45,100, respectively.

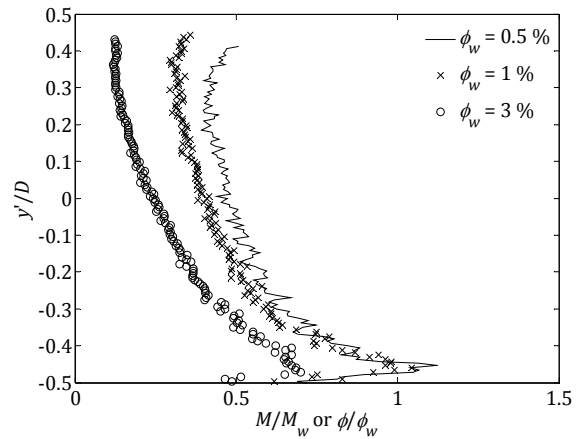

Figure 2: Particle concentration versus distance from centreline (normalised) with large glass spheres (d_{50} = 77 μm) at three nominal (weighed) concentrations. Re = 44,400, 44,600 and 44,200, respectively.

The particle concentration is most strongly underestimated at higher concentrations (ϕ_w = 1

% and 3 %) for the two plastic species (Figure 3 and Figure 4). This is caused by high attenuation – which, as expected, is more significant for the plastic particles than the glass species, since they are considerably larger – and illustrates a number of important points relating to industrial application of this method: first, that the ultrasonic frequencies must be chosen carefully such that attenuation is minimised (which in practice means using lower frequencies); and second, that for a particular particle species there exists an effective limiting concentration above which a suspension thereof becomes acoustically opaque (in the range $0 < \phi_w < 1$ %, in the case of the plastic species used here, for example).
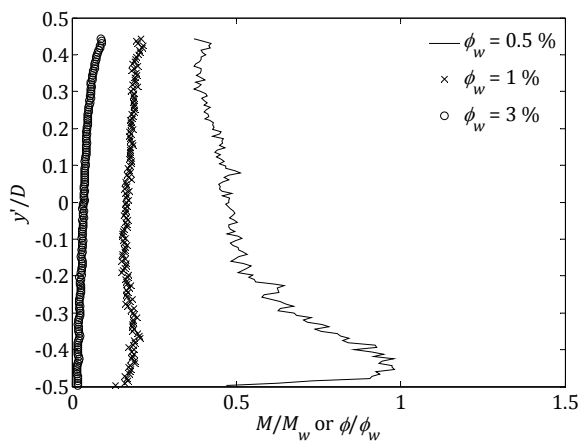

Figure 3: Particle concentration versus distance from centreline (normalised) with small plastic beads (d_{50} = 468 μm) at three nominal (weighed) concentrations. Re = 45,200, 44,700 and 44,300, respectively.
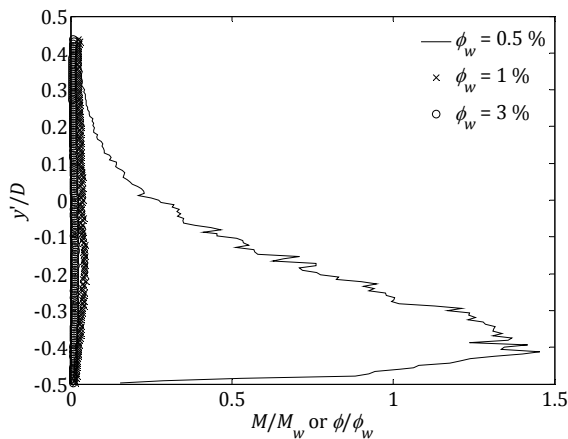

Figure 4: Particle concentration versus distance from centreline (normalised) with large plastic beads (d_{50} = 691 μm) at three nominal (weighed) concentrations. Re = 43,000, 43,300 and 42,100, respectively.

4 Results: Settling flows

Concentration profiles, RMS echo voltage profiles and settled bed depths are presented for two case studies at Re = 25,000. Results for Case 1, for large glass spheres at ϕ_w = 3 %, are presented in Figure 5 (RMS echo voltage profiles) and Figure 6 (concentration profiles, with bed depths indicated). The corresponding results for Case 2, small plastic beads at ϕ_w = 1 %, are shown in Figure 7 and Figure 8, respectively. Note that, as in the figures presented in Section 3, the axes are orientated so as to aid visualisation.

First, the results for Case 1 are described. Figure 5 shows the RMS echo voltage, V, from the transducer perpendicular to the flow direction and pipe walls (4 MHz) for two runs, one with flow, and another immediately following the first, but with the flow stopped ("stop-flow" run). Both show clear peaks, the positions of which are overlaid on a plot of the computed particle concentration, M (via Eq. (7)) in Figure 6.

By inspection of Figure 6, a peak is present in the computed particle concentration, M, centred at y'/D = -0.326, although it is quite broad and covers approximately a region of $0.3 < y'/D < 0.4$. It can be seen from Figure 5 that there is a peak in the RMS echo voltage, V, at y'/D = -0.370 (dashed line in both figures) and the settled bed surface is at y'/D = -0.335 (dashed-dotted line).
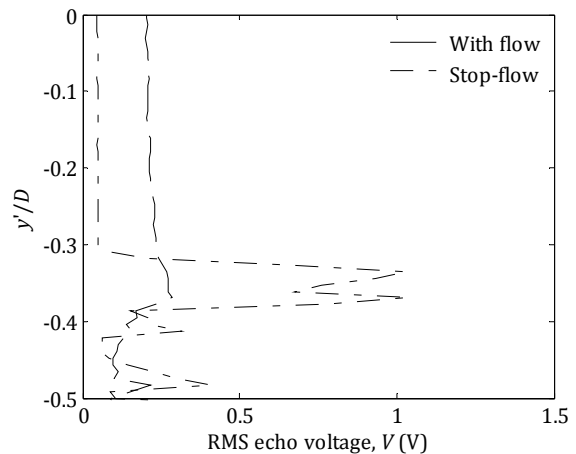

Figure 5: RMS echo voltage, V, versus distance from centreline (normalised) with large glass spheres (d_{50} = 77 μm) at ϕ_w = 3 %. Re = 25,000. Dashed lined: with flow; dashed-dotted line: flow ceased ("stop-flow"). Only lower half of flow shown.
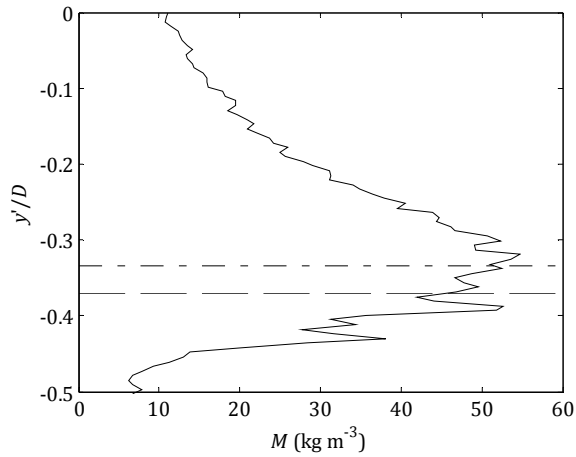
Figure 6: Particle concentration versus distance from centreline (normalised) with large glass spheres (d_{50} = 77 µm) at ϕ_w = 3 %. Re = 25,000. Dashed lined: position of peak in RMS echo voltage; dashed-dotted line: position of settled bed surface upon cessation of flow, both as in Figure 5. Only lower half of flow shown.
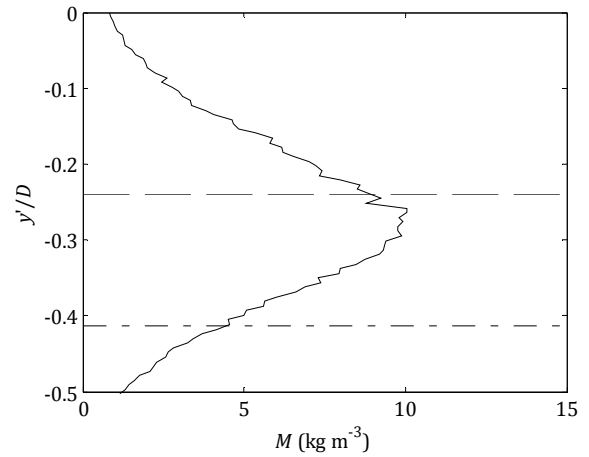
The corresponding results for Case 2 are shown in Figure 7 (RMS echo voltage, V, with and without flow) and Figure 8 (concentration profile with RMS echo peak positions overlaid). It can be seen from Figure 8 that there is a peak in M centred at y'/D = -0.276, although it is very broad, covering most of the lower half of the pipe flow, *i.e.* the domain shown. A peak in the RMS echo voltage, V, is also evident in Figure 7 at y'/D = -0.239 (dashed line) and the surface of the settled bed is at y'/D = -0.413 (dashed-dotted line).
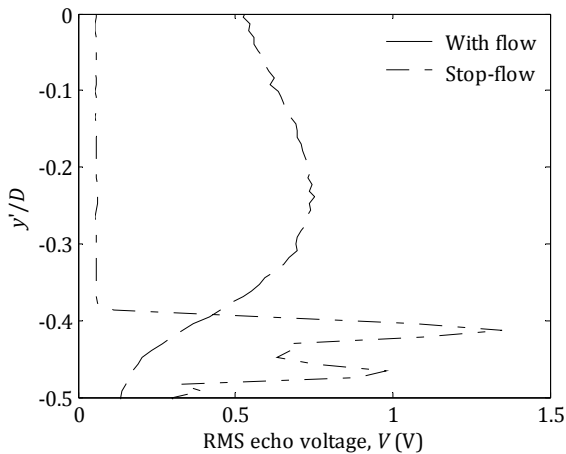

Figure 7: RMS echo voltage, V, versus distance from centreline (normalised) with small plastic beads (d_{50} = 468 µm) at ϕ_w = 1 %. Re = 25,000. Dashed lined: with flow; dashed-dotted line: flow ceased ("stop-flow"). Only lower half of flow shown.

Figure 8: Particle concentration versus distance from centreline (normalised) with small plastic beads (d_{50} = 468 µm) at ϕ_w = 1 %. Re = 25,000. Dashed lined: position of peak in RMS echo voltage; dashed-dotted line: position of settled bed surface upon cessation of flow, both as in Figure 7. Only lower half of flow shown.

In general, the received RMS echo voltage would be expected to reach a peak within the shear layer or moving bed region. Physically speaking, the position of the peak in the echo voltage indicates the point at which acoustic energy is backscattered most strongly. The acoustic signal in any multiphase flow is subject to two competing processes: absorption and scattering. When measured with a monostatic transducer, these processes manifest themselves as attenuation and backscatter strength, and both have different dependences on particle properties (see Section 2.1) and distance from the transducer, such that the peak in the echo voltage corresponds broadly to the point at which attenuation overcomes backscattering. The results for both case studies are consistent with this expectation. However, the structure of the echo voltage profiles relative to the computed concentration profiles and settled bed depths requires more interpretation.

With reference to the attenuation coefficients listed in Table 1, the suspension in Case 1 (glass spheres, d_{50} = 77 µm) was much less attenuating than that in Case 2 (plastic beads, d_{50} = 468 µm). As a result, and despite the lower nominal concentration in Case 2 (ϕ_w = 1 %) relative to Case 1 (ϕ_w = 3 %), the peak in the echo voltage was much higher in the flow in Case 2 than in Case 1, and well above the position of the peak in the computed particle concentration, M. The opposite was found in Case 1: the peak in the echo voltage fell below the peak in M.

It is also important to note that the flow velocity in both cases was the same (Re = 25,000) and so, notwithstanding the difference in nominal

particle concentrations, any differences in the flow structure would be expected to be caused by particle size and therefore the tendency of the particles to settle. For this reason, it is interesting to observe that V in Case 1 peaks much lower in the flow than in Case 2, despite a higher nominal concentration. This, again, can be explained by the attenuation being much lower in Case 1.

Lastly, it is clear by comparing the dashed-dotted lines in Figure 6 (Case 1) and Figure 8 (Case 2) that the settled bed thickness in Case 1 is greater than that in Case 2, as would be expected: the nominal concentration, and therefore the cross-sectional area occupied by settled particles, is greater in Case 1 (ϕ_w = 3 %) than in case 2 (ϕ_w = 1 %). Less intuitively, however, it is seen in Case 1 that the positions of the peaks in V and M occur relatively close to the settled bed surface in the stop-flow run, suggesting that the acoustic signal penetrates well into the moving part of the bed and is attenuated only at the interface with the stationary part of it, whereas in Case 2 the peaks in both M and V occur well above the surface of the settled bed. The conclusion to be drawn from this observation is that the acoustic signal can penetrate deep into the shear layer/moving bed region for weakly attenuation suspensions (*e.g.* Case 1), but is absorbed well above that region in more strongly attenuating suspensions (*e.g.* Case 2).

5 Conclusions

The models of Thorne and Hanes (2002) and Hurther *et al.* (2011), for which data only exist for quartz-type sand, have been adapted for particles of arbitrary physical properties. Measured values of the backscatter and attenuation coefficients for four particle species with different physical properties were presented, and concentration profiles over a range of nominal concentrations in horizontal pipe flow were given. Both the values of the coefficients and the concentration profiles themselves followed the expected trends.

The concentration measurement method presented here, which is novel as a whole, has great potential for measuring the settling and segregation behaviour of real suspensions and slurries in a range of applications where in-situ characterisation is required, such as the nuclear and minerals processing industries. It is intended that the ξ_h and K_h data presented here will form the basis of a larger database of backscatter and attenuation coefficients for sediments commonly encountered in a range of engineering industries.

The comparison of complementary concentration profiles, echo voltage data and bed depth results make it clear that the suite of acoustic methods presented here can be used to interrogate complex flows in a very detailed manner, and demonstrate the flexibility of the methods and their potential in a range of industries.

References

Hurther, D., Thorne, P.D., Bricault, M., Lemmin, U. and Barnoud, J.M. (2011), A multi-frequency acoustic concentration and velocity profiler (ACVP) for boundary layer measurements of fine-scale flow and sediment transport processes. *Coast. Eng.*, Vol. 58, pp. 594-605.

Rice, H.P. (2013), Transport and deposition behaviour of model slurries in closed pipe flow, Ph.D. thesis, University of Leeds.

Rice, H.P., Fairweather, M., Hunter, T.N., Mahmoud, B., Biggs, S.R. and Peakall, J. (2014), Measuring particle concentration in multiphase pipe flow using acoustic backscatter: Generalization of the dual-frequency method, in press. *J. Acoust. Soc. Am.*, DOI: 10.1121/1.4883376.

Thorne, P.D. and Hanes, D.M. (2002), A review of acoustic measurement of small-scale sediment processes. *Cont. Shelf Res.*, Vol. 22, pp. 603-632.

Thorne, P.D. and Meral, R. (2008), Formulations for the scattering properties of suspended sandy sediments for use in the application of acoustics to sediment transport processes. *Cont. Shelf Res.*, Vol. 28, pp. 309-317.